Figure S1

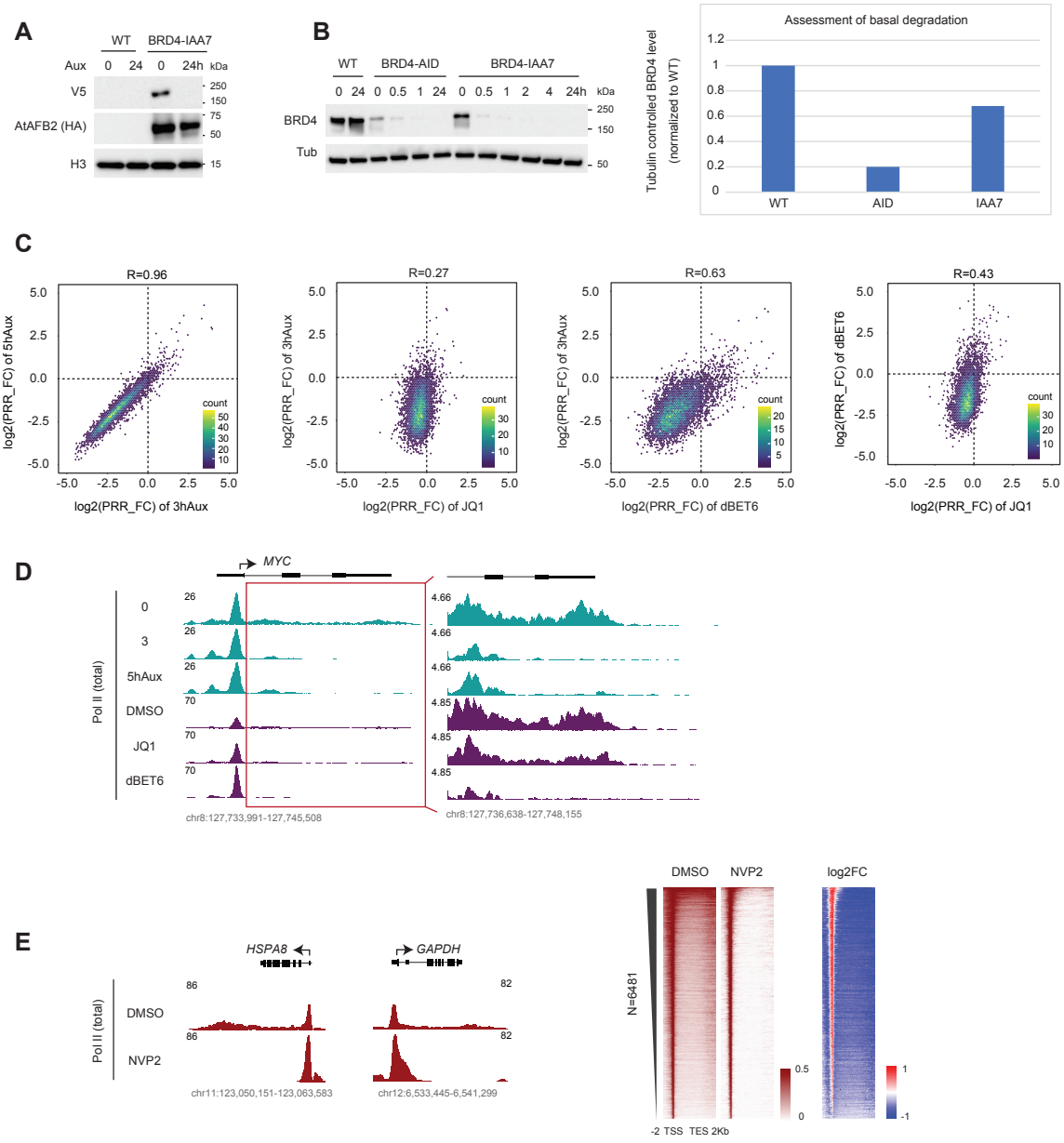

Figure S1. Differences in Pol II pausing induced by BRD4 depletion and bromodomain inhibition, related to Figure 1

A. Western blot showing the expression of HA-tagged AtAFB2 and the auxin-induced degradation of V5-tagged BRD4 using anti-tag antibodies.

B. Western blot comparing the BRD4 protein expression level and degradation kinetics of the previously published BRD4-AID degron[12] to those of the BRD4-IAA7 degron used in this study (left). Basal degradation of the BRD4 protein in the two systems were assessed by comparison of the percentage of the tubulin-normalized protein level relative to WT in each group (right). Note: in Figures S1A and S1B, the BRD4-IAA7 clone used is D4 (Hygromycin selected); it is G3 (Neomycin selected) otherwise in the study.

C. Scatter plot of the gene-by-gene PRR correlations between auxin treatment durations and between JQ1 and auxin, dBET6 and auxin, or JQ1 and dBET6 treatment (normalized to corresponding vehicles).

D. Track examples of Pol II ChIP-seq signal at the MYC locus upon auxin treatment (0, 3 or 5h), JQ1 or dBET6 treatment (3h) with a zoom-in view at the gene body.

E. Track examples of Pol II ChIP-seq signal at the HSPA8 and GAPDH loci upon NVP-2 treatment (2h) and corresponding heatmaps showing Pol II occupancy profiles and fold change in occupancy vs control upon NVP-2 treatment.

Figure S2

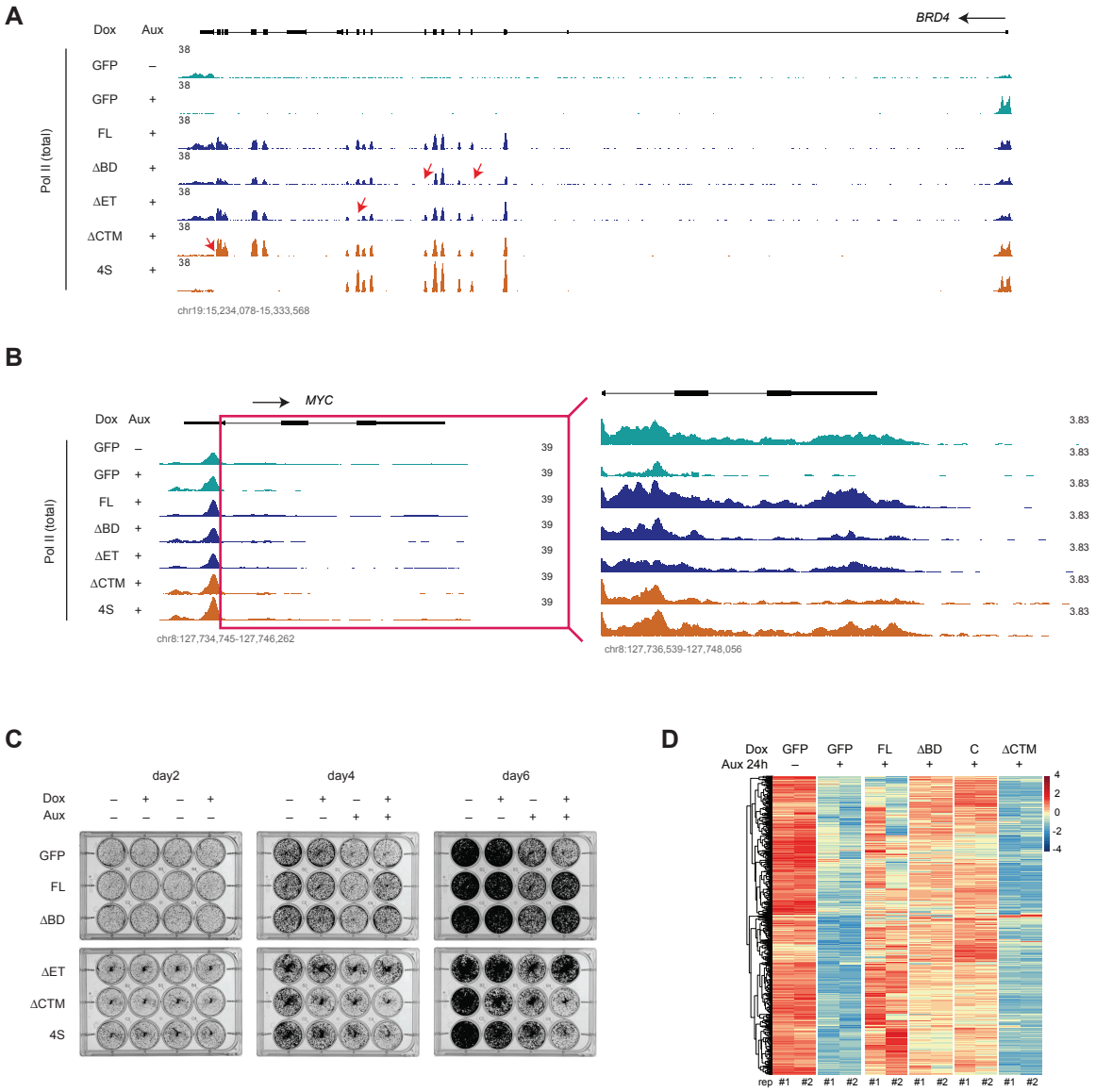

Figure S2. BRD4 depletion and rescue by different mutants, related to Figure 2

A. Tracks of the total Pol II ChIP-seq signal at the BRD4 gene locus in the rescue experiment with the arrows indicating the loss of exonic signal corresponding to mutant sequence.

B. Tracks of the total Pol II ChIP-seq signal at the MYC gene locus as well as the genebody zoom in for different mutant rescue upon auxin treatment.

C. Plate images showing cell growth over the time course of BRD4 depletion and mutant complementation.

D. RNA-seq log2(x+1) scaled counts (UQ-corrected) reveal a subset of genes (N=863) that were rescued by bromodomain-less BRD4 mutants but not the ΔCTM mutant upon depletion of endogenous BRD4 for 24h.

Figure S3

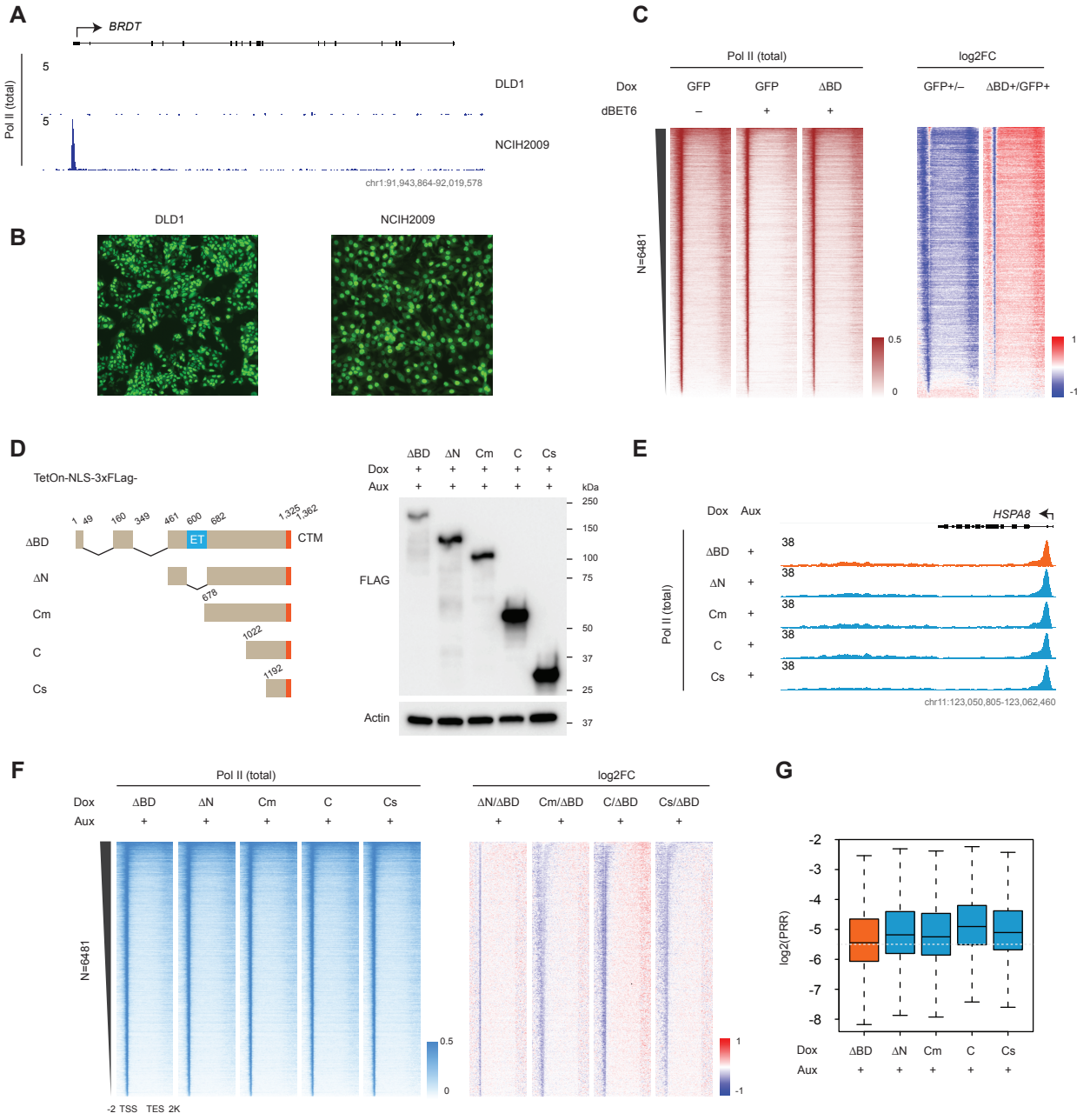

Figure S3. Bromodomain-less BRD4 expression in NCIH2009 cells and the screen for a minimal CTM-containing fragment in DLD-1 cells, related to Figure 3

A. Tracks comparing the Pol II ChIP-seq signal at the BRDT gene locus in DLD-1 and NCIH2009 cells.

B. Fluorescent images comparing the expression of GFP control in the DLD-1 and NCIH2009 cells.

C. Heatmap showing the genome-wide Pol II occupancy and the corresponding fold changes for the dBET6 treatment and rescue by ΔBD complementation in NCIH2009 cells.

D. Schematic of the FLAG-tagged, bromodomain-less BRD4 mutant constructs, with western blot showing protein expression upon Dox treatment (2d) in BRD4-IAA7 cells.

E. Track examples of the total Pol II ChIP-seq signal upon auxin treatment in BRD4-IAA7 cells expressing the FLAG-tagged mutants in D.

F. Heatmap of the genome-wide Pol II occupancy profile from the Pol II ChIP-seq in E and the corresponding fold changes in occupancy relative to ΔBD.

G. Boxplot showing the log2PRR for the conditions in E.

Figure S4

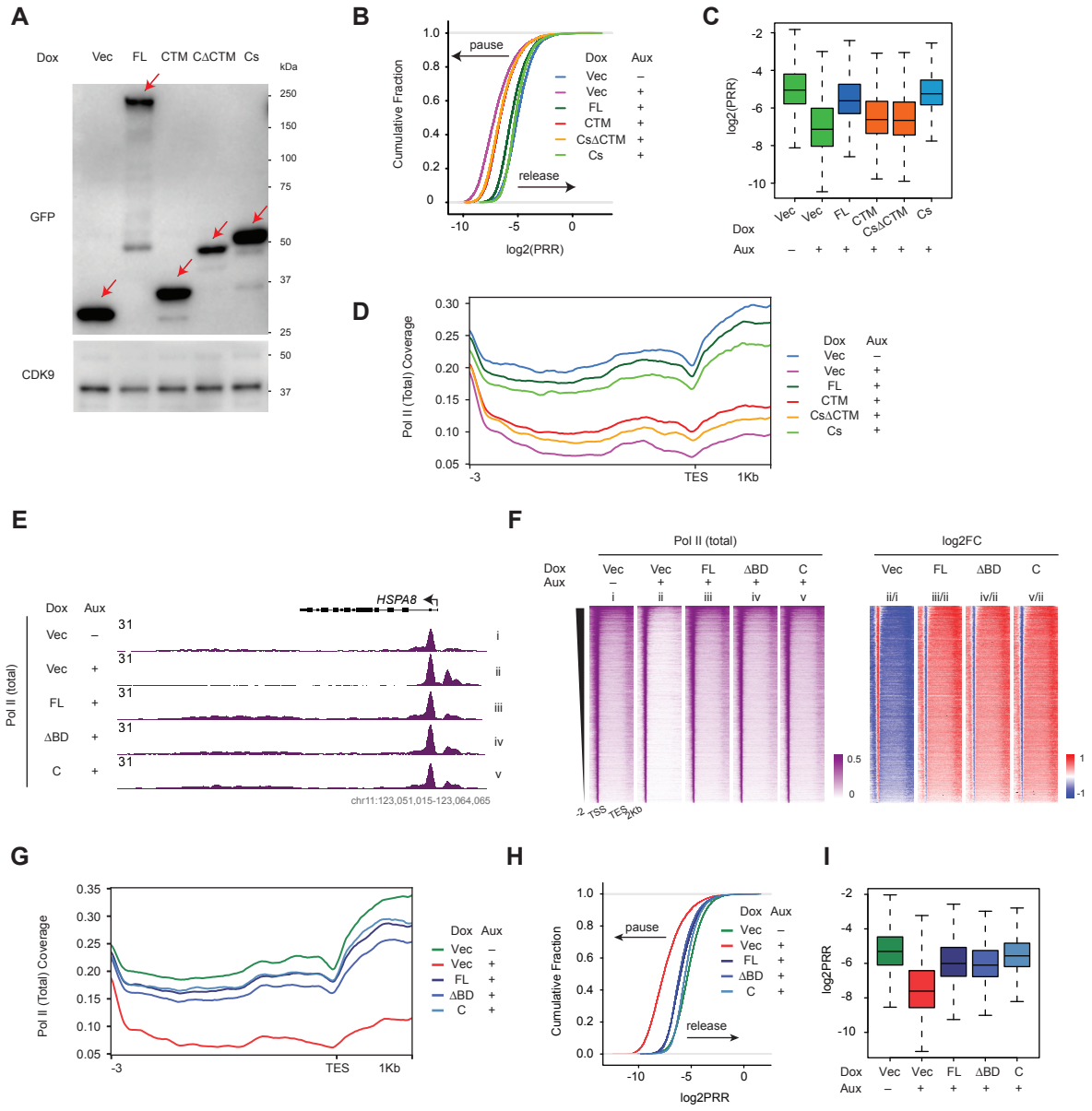

Figure S4. BRD4 C terminal fragments interact with PTEFb and release paused Pol II, related to Figure 4

A. Western blot showing the expression of GFP-tagged FL BRD4 or the CTM, CsΔCTM or Cs mutant constructs upon Dox induction (2d.) (Vector: TetOn-NLS-GFP).

B. ECDF showing the log2PRR from the Pol II ChIP-seq for the rescue experiment in Figure 4E.

C. Boxplot showing the log2PRR from the Pol II ChIP-seq for the rescue experiment in Figure 4E.

D. Metagene plot showing Pol II occupancy around the TES as a reference point, for the Pol II ChIP-seq conditions in Figure 4E.

E. Track examples showing the total Pol II ChIP-seq signal for BRD4 depletion and rescue with indicated mutants.

F. Heatmap showing the genome-wide Pol II occupancy profiles and the corresponding fold changes for the conditions in E.

G. Metagene plot showing the Pol II occupancy profile, around the TES as a reference point, from the Pol II ChIP-seq for conditions in E.

H. ECDF showing the log2PRR from the Pol II ChIP-seq for conditions in E.

I. Boxplot showing the log2PRR from the Pol II ChIP-seq for conditions in E.

Figure S5

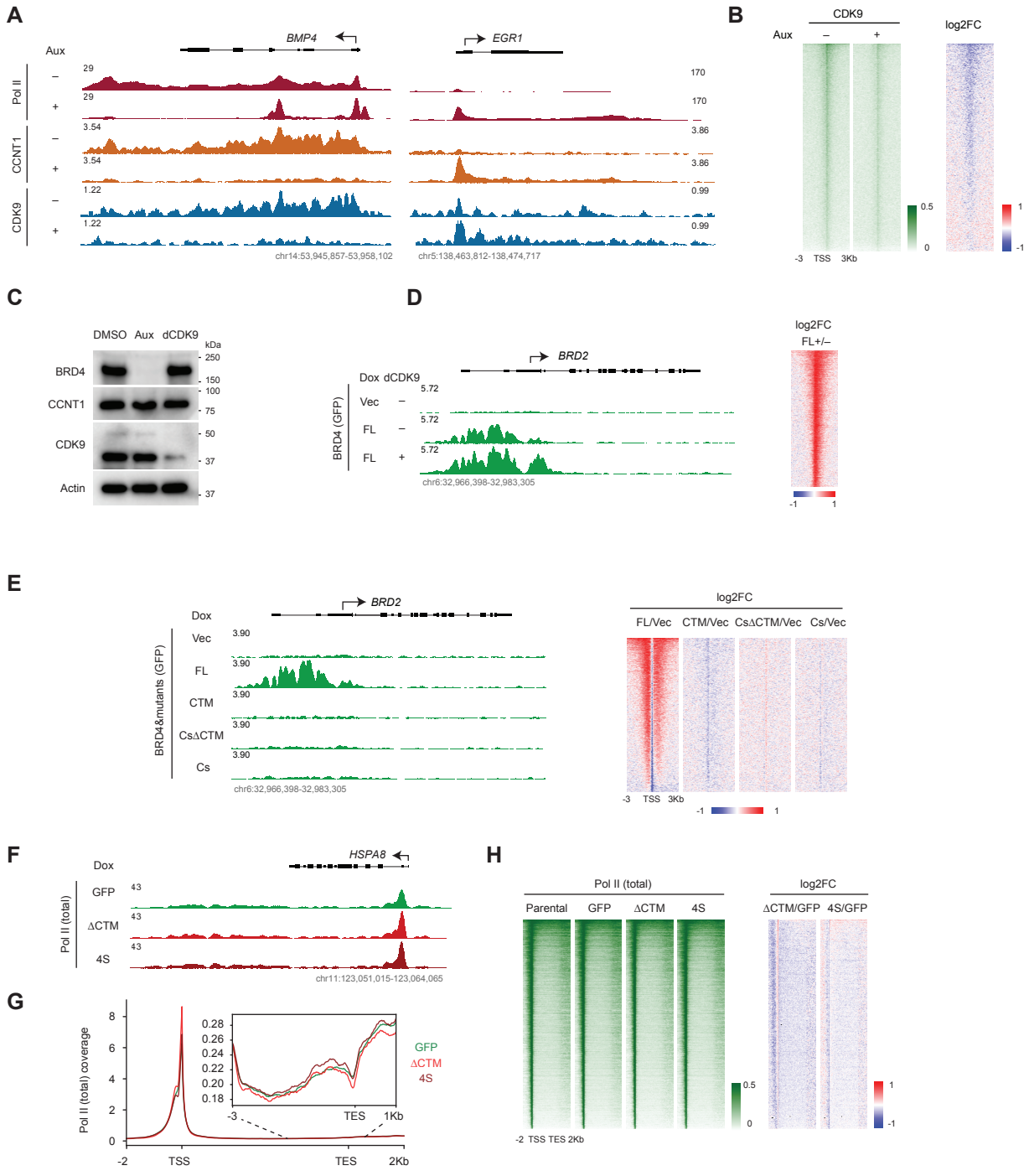

Figure S5. Genome-wide PTEFb binding relies on BRD4 association with histone acetylation, related to Figure 5

A. Track examples comparing the ChIP-seq signals for Pol II, CCNT1 and CDK9 in the same samples of auxin-treated (3h) BRD4-IAA7 cells.

B. Heatmap showing the genome-wide CDK9 occupancy and the corresponding fold change upon auxin treatment for the condition in A. Genes are ranked by CDK9 signal in control.

C. Western blot showing stable PTEFb protein levels upon depletion of BRD4 by auxin treatment, and degradation of CDK9 but not CCNT1 or BRD4 upon dCDK9 (2.5uM) treatment for 3h in BRD4-IAA7 cells.

D. Track examples for GFP ChIP-seq signal at the BRD2 gene locus upon Dox-induced expression of GFP-tagged BRD4-FL with or without dCDK9 treatment (left). Heatmap showing the genome wide GFP-BRD4-FL occupancy fold change upon dCDK9 treatment (right), ranked by GFP signal in the untreated GFP-BRD4-FL condition. Endogenous BRD4 was depleted by auxin treatment for 2h prior to the addition of dCDK9.

E. Track example for GFP ChIP-seq upon induction of GFP-tagged BRD4-FL or the indicated mutants (left). Heatmap showing the genome-wide fold changes of the GFP-tagged BRD4 FL and mutant constructs relative to the vector (right). The endogenous BRD4 is depleted by auxin treatment for 3h across all samples. Genes ranked by GFP signal in the GFP-BRD4-FL condition.

F. Track examples of Pol II ChIP-seq signal upon Dox induction for the CTM-less BRD4 mutants. This experiment was carried out concurrently with the rescue experiment in Figure 2. The GFP condition in Figures 2C and 2D was used here as a control.

G. Metagene plot showing the Pol II occupancy for the conditions in F with a zoom-in view around the TES as a reference point.

H. Heatmap showing the genome-wide Pol II occupancy profiles and the corresponding fold changes for the conditions in F.

Figure S6

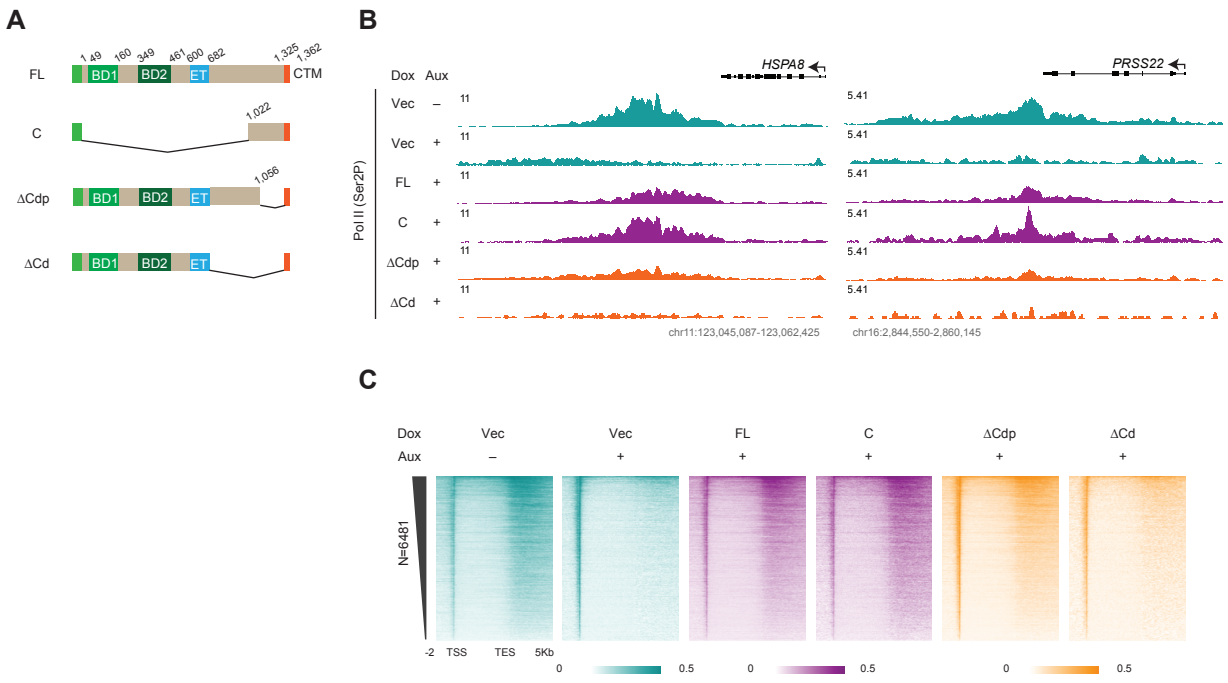

Figure S6. BRD4 C-terminus stabilizes PTEFb and confers Pol II CDT phosphorylation activity, related to Figure 6

A. Schematic of the GFP-tagged BRD4-FL, BRD4-C and two versions of BRD4-ΔCd (partial and total deletion of the C-terminal disordered region).

B. Track examples of the Ser2P ChIP-seq signal upon BRD4 depletion and rescue by the two versions of BRD4-ΔCd. This experiment was carried out concurrently with the rescue experiment in Figure 4. The Vec –/+ Auxin conditions in Figures 4G and 4H were used here as control.

C. Heatmap showing the genome-wide Ser2P occupancy for the conditions in B.

Table S1. Myc-like genes that are rescued by FL but not ΔBD, related to Figure 2

49 genes that met a less stringent cutoff for rescue by FL but not ΔBD (log2FC of PRR FLvsΔBD >=0.585 & log2FC of Pol II occupancy FLvsΔBD >=0.585).

Gene	ID	Chr	PRR_log2FLvsΔBD	genebody_log2FLvsΔBD
SYT8	ENSG00000149043.17	chr11	2.159992789	1.783530576
CXCL5	ENSG00000163735.7	chr4	1.487619501	1.567082964
ALDH1A3	ENSG00000184254.17	chr15	0.602975124	1.442493658
EN2	ENSG00000164778.4	chr7	0.705392511	1.214393043
VIPR1	ENSG00000114812.13	chr3	0.913809478	1.17267642
MYC	ENSG00000136997.21	chr8	1.052547361	1.143905835
WASHC2A	ENSG00000099290.17	chr10	0.655929022	1.134605017
KRT80	ENSG00000167767.14	chr12	1.168665542	1.100289237
ISOC2	ENSG00000063241.8	chr19	0.969626351	1.050499384
PRSS23	ENSG00000150687.12	chr11	0.84434861	1.049689133
IFT22	ENSG00000128581.17	chr7	0.908792686	1.005922998
NOL6	ENSG00000165271.17	chr9	0.855300847	0.953015127
ALDH1B1	ENSG00000137124.8	chr9	0.635422187	0.943146854
PNPO	ENSG00000108439.11	chr17	0.676632082	0.86690695
CCND1	ENSG00000110092.4	chr11	0.973576229	0.855707485
MRPL15	ENSG00000137547.9	chr8	0.845082945	0.854861369
DBNDD1	ENSG00000003249.15	chr16	0.790886418	0.845408124
LAD1	ENSG00000159166.15	chr1	0.596866416	0.830407301
GDF15	ENSG00000130513.7	chr19	0.952055912	0.814050263
TGFB2	ENSG00000092969.12	chr1	0.648091982	0.808104192
GHDC	ENSG00000167925.16	chr17	0.857263493	0.803399108
DDX21	ENSG00000165732.14	chr10	0.606893199	0.79778035
DDX56	ENSG00000136271.11	chr7	0.671335409	0.77872959
CCDC22	ENSG00000101997.13	chrX	0.761567567	0.777271586
IL36RN	ENSG00000136695.15	chr2	1.11883623	0.772034937
MYB	ENSG00000118513.20	chr6	0.641361793	0.765698475
LGALS3BP	ENSG00000108679.13	chr17	0.791261752	0.764930551
ZNF771	ENSG00000179965.12	chr16	0.647275294	0.762225414
METTL7A	ENSG00000185432.12	chr12	1.183797176	0.759434901
CYP1A1	ENSG00000140465.15	chr15	1.421527767	0.752769078
HMG20B	ENSG00000064961.19	chr19	0.763469976	0.736173439
MCM2	ENSG00000073111.14	chr3	0.667495869	0.727087531
MVB12A	ENSG00000141971.13	chr19	0.718113228	0.723125337
NOLC1	ENSG00000166197.17	chr10	0.697748882	0.693588451
RBBP8NL	ENSG00000130701.4	chr20	0.604868722	0.679830792
CHMP6	ENSG00000176108.9	chr17	0.627327886	0.679271047
SETD1B	ENSG00000139718.12	chr12	0.806746275	0.677526151
MCM5	ENSG00000100297.16	chr22	0.754325631	0.674936249
ALDH7A1	ENSG00000164904.18	chr5	0.611537845	0.667712821
METTL13	ENSG00000010165.20	chr1	0.934505679	0.653979176

MARC1	ENSG00000186205.13	chr1	1.172704878	0.650556711
GTF3C6	ENSG00000155115.7	chr6	0.675162347	0.649060893
LDHB	ENSG00000111716.14	chr12	0.614782298	0.642948781
BMP4	ENSG00000125378.16	chr14	0.75936461	0.635414596
SNORD82	ENSG00000115053.17	chr2	0.595052277	0.623364254
ANXA1	ENSG00000135046.14	chr9	1.08246216	0.620031844
CDK4	ENSG00000135446.17	chr12	0.800086922	0.620031844
DTD2	ENSG00000129480.13	chr14	0.64458806	0.597664031
DNAL4	ENSG00000100246.13	chr22	0.592822558	0.585036423